

國立臺灣大學醫學院暨工學院醫學工程學研究所

碩士論文

Institute of Biomedical Engineering  
College of Medicine and Engineering  
National Taiwan University  
Master Thesis

以具方向性的膠原蛋白模型  
來探討細胞在立體空間中之運動  
An Aligned 3D Collagen Matrix  
for the Study of Cell Migration



馮嘉襄

Chia-Hsiang, Feng

指導教授：趙本秀 博士

Advisor: Pen-Hsiu Chao, Ph.D.

中華民國 100 年 7 月

June, 2011

國立臺灣大學（碩）博士學位論文  
口試委員會審定書

具方向性的膠原蛋白模型來探討細胞在立體空間中之運動  
A Novel Aligned 3D Collagen Matrix for the Study of Cell Migration

本論文係馮嘉襄君（R98548058）在國立臺灣大學醫工所學系、  
所完成之碩（博）士學位論文，於民國一百年七月十八日承下列考試  
委員審查通過及口試及格，特此證明

口試委員：

趙平

（指導教授）

郭柏崧

林榮輝

所長：

工學院醫工所所長楊台鴻

## 誌謝

我要首先感謝我的指導教授，趙本秀老師，這兩年來的對我的指導。在研究方面老師很早就和我討論出方向，讓我能盡早準備並有所成果。也感謝他讓我能有去企業實習的機會，對於我的眼界以及發展都助益良多。感謝我的口試委員林峰輝教授和郭柏齡教授，在口試時給予我的指導以及鼓勵。感謝生科院的陳香君教授、朱蔡豈博士、以君、亞臻幫助我解決很多免疫染色以及生物實驗操作上的問題。還有感謝實驗室的同學，維仁、祐甄、新民、承憲、沿毓、守謙、向儀，陪伴我的實驗室生活，為我的最後的學生生涯畫上精彩的句點。最後感謝我的家人，在我的碩士生活中給我的照顧以及鼓勵，讓我能充實自己，為未來做好準備。



## 中文摘要

本實驗的目標是要發展出一個有方向性的膠原蛋白模型來探討韌帶纖維母細胞在三度空間中之移動。韌帶纖維母細胞原生在由膠原蛋白纖維束組成的排列結構中，而研究顯示具方向性的環境可以改變細胞外型，蛋白表現、細胞移動和附著。同時，細胞在平面上和三度空間之中會表現出不同的細胞表現。在本實驗中，我們利用微流道的方式創造出一個有排列的膠原蛋白，來比較細胞在平面和三度空間中的差異。我們施加電場在細胞來提供一個均勻的刺激。

細胞在平面和三度空間中都顯現出對於有方向性的膠原蛋白會排列，同時在電刺激下會沿著膠原蛋白的纖維走向移動爬行。但是，細胞移動的方向性似乎也受到了膠原蛋白的高度影響。這個影響可能跟細胞附著的調節和細胞張力恆定有關。

關鍵字：細胞爬行，三度空間膠原蛋白，張力恆定，電刺激

# Abstract

The aim of this study is to develop an aligned collagen matrix to examine cell migration of ligament fibroblasts, which natively reside in a highly collagen fibrous and anisotropic microenvironment made of type I collagen. This highly aligned arrangement has been shown to modulate fibroblast morphology, migration rate and attachment. However, cells also exhibit significantly different behaviors in 2D and 3D environments. In the current study, a microfluidic device was developed to create aligned collagen hydrogel and examine cell migration behavior in 2D and 3D collagen matrix. Cells are subjected with an electrical field to apply a homogenous field of migration stimulation.

Cells in both 2D and 3D show high alignment to the collagen matrix and cell migration show preference of contact guidance over EF stimulation. However, cell migration directionality is influenced by matrix thickness, possibly through regulation of cell attachment disassembly and tensional homeostasis.

Key Word: Cell migration, 3D collagen matrix, tensional homeostasis, electrical field

# Contents

口試委員會審定書.....	i
誌謝.....	ii
中文摘要 .....	iii
Abstract .....	iv
Chapter 1 Introduction	
1.1 Cell migration .....	1
1.2 Cellular microenvironment.....	4
1.3 Hypothesis: Matrix stiffness affects cell migration in aligned collagen matrix.....	6
Chapter 2 Materials and Methods	
2.1 Cell Culture .....	9
2.2 Microchannel Fabrication .....	10
2.3 Collagen Preparation.....	10
2.4 Electric Field Studies.....	13
2.5 Cell Morphology and Migration Analysis.....	13
2.6 Scanning Electrical Microscopy .....	14
2.7 Immunofluorescence Microscopy .....	14
2.8 Statistical analysis.....	15

Chapter 3	Results.....	17
Chapter 4	Discussion .....	23
Reference	.....	39
Appendix.....		44



# List of Figures

Figure 1A. Pattern of microchannel.....	29
Figure 1B. Bifurcation at the inlets of the main channel.....	29
Figure 1C. Dimensions of PDMS microchannel.....	29
Figure 2A. Procedure of preparing 3D aligned collagen samples.....	30
Figure 2B .Procedures of preparing a doubled layer 3D sample .....	30
Figure 3. Cross-sectional image of different collagen sample and cell morphology.....	31
Figure 4A. Components of the electrical stimulation chamber.....	32
Figure 4B. Connection of electrical stimulation.....	32
Figure 5. SEM of collagen fibril.....	33
Figure 6A. ACLF in random collagen .....	34
Figure 6B. ACLF in aligned collagen.....	34
Figure 6C. Collagen fibril angle distribution.....	34
Figure 6D. Total percentage of collagen fibril angle within $\pm 15$ degrees. ....	34
Figure 7 Cell orientation distribution.....	35
Figure 8A Examples of cell migration under EF stimulation—.....	36
Figure 8B Table of percentage of cells that undergo detach during a 2 hr EF study and	



Pearson correlation coefficient of actin and tubulin co-localization.....	36
Figure 8C Polar charts of cells under EF stimulation—.....	36
Figure 9A Directional velocity of ACLF toward cathode.....	37
Figure 9B Migration speed of ACLF.....	37
Figure 10A Comparison of directional velocity of Y2736 treated ACLFs cell migration .....	38
Figure 10A Comparison of migration speed of Y2736 treated ACLFs cell migration .....	38



# Chapter 1

## Introduction

### 1. Cell migration

Cell migration is an important behavior for multicellular organisms. During embryonic development, cells migrate and proliferate to form tissues. One example is the migration of neural crest cells, which leave the neural tube during development, migrate to other region and differentiate into tissues such as the peripheral nervous system. Cell migration plays a major role in for wound healing. For example, if a bone fractures, chondroblasts followed by osteoblasts will migrate into the fractured area to proliferate and differentiate separately into chondrocytes and osteocytes, either to produce a cartilaginous or bony matrix to fill in the wound. At the wound site, macrophages can migrate through tissue to engulf bacteria at the infection spot, just as fibroblasts can migrate though connective tissue to remodel and repair damaged tissue. Cell migration is also important in cancer metastasis, where cancer cells penetrate into blood and lymph vessels to transport and spread. Cell migration has been studied in vitro. Most of these studies seed cells on glass slides or Petri dishes to monitor their activities.

Cell migration, is generally modeled as a three step process [1]. At the first stage,

polarization, the cell polarizes into front and rear side and performs different molecular process at each side. For example, in some cells, the microtubule organizing center (MTOC) and Golgi apparatus are localized between the front side and the nucleus. This orientation is possible to support the intensive vesicle transportation from the Golgi apparatus toward the front edge. Several proteins are also incorporated in polarization, especially cdc42, which is considered “ master regulator of cell polarity. [1]” Cdc42 is found active in the front edge, and influences lamellipodia formation and MTOC localization [2]. As for the rear side, signal factors like Rho are found. Rho is related to cell contraction, in which inhibiting Rho usually leads to extended tail [3].

In the second phase, protrusion and adhesion, the front side of a cell first forms protrusions that extend out of the cell body. These protrusions, which can be classified as lamellipodia or filopodia, are supported by actin polarization. The actin network usually shows an orthogonal array in a lamellipodia, in contrast to the tightly packed, parallel bundle of actin found in filopodia [4]. These protrusions are further stabilized by adhesion with the extracellular matrix (ECM). Although adhesion involves several kinds of proteins, integrins are the major receptor family that bind and react to the outside world during migration. The integrin is composed with two sub chains:  $\alpha$  chain and  $\beta$  chain [5]. Each of these two chains have sub families that allows mix matching

between the two, forming different kinds of integrin combinations to recognize different ECM surroundings. Integrin in some cases cluster with other proteins to form focal complexes, or sometimes even more mature, larger assemblies called focal adhesion [6]. Focal adhesion is a protein complex that connects the ECM to the cell's cytoskeleton. In a focal adhesion, the ECM binds with integrin, which binds with protein such as talin, vinculin and focal adhesion kinase that connects with the actin cytoskeleton. Focal adhesions serve as anchors during cell migration as cells contract or extend themselves over the ECM.

In the final stage, contraction, the cell must first detach the adhesion at the rear edge and then apply a force to pull on adhesion on the front edge and so to advance. This contraction force mainly derives from myosin II activity, which is regulated by MLC kinase (MLCK) and Rho kinase (ROCK) [1].

Cell migration is inducible via chemical or physical stimulation. Cells can be orientated by a chemical gradient, as cells tend to migrate toward higher or lower concentrations depending on the stimulation. This phenomenon is found both in vitro, for example cells have been shown to migrate toward higher glucose concentrations [7], and in vivo, as cells during embryonic development are shown to respond and communicate with chemical signals, creating specific tissue structures [8]. Cells also

response to physical stimulations like electric field (galvanotaxis) [9] or stiffness gradients (durotaxis)[10, 11]. For example, fibroblasts seeded on a glass slide are shown to migrate toward the cathode under an electrical field [10].

## **2. Cellular microenvironment**

Cell migration on a glass slide or Petri dishes has been studied for decades, yet cells in vivo reside in not only a 3 dimensional but also a structural environment. For example, connective tissue such as skin, cartilage, tendon and ligament all base on collagen to form their structure and provide strength. Although these tissue are mostly composed by the same protein: collagen fibrils, these fibrils from different structures to serve different functions. Collagen fibrils in skin appear as a cloth like structure, as fibrils interweave with each other. In contrast, collagen fibrils in mature bones and cornea show “orderly plywoodlike layers” as fibrils in each layer do not interweave, but each layer stacks on each other perpendicularly. Collagen fibrils in ligament and tendon form parallel bundles and fascicles, a structure to resist tension along the major axis. Ligament and tendon collagen fibrils also exhibit planar and helical “crimp-like” structures [11] for absorbing shocks and providing flexibility.

In fact, structural environment has been shown to affect cell behavior. For example,

aligned matrices are common in animal tissue, and have been shown to effect cell alignment, migration and protein expression. Cells seeded on nano groves etched on a quartz substrate show alignment and migration along the direction of the groves, a phenomenon named as contact guidance [12]. Doyle and coworkers have also used microcontact printing to create linear pattern for cell seeding, and shown that cells tend to align and migrate along these patterns [13]. Previously, we have shown that when ligament fibroblasts are seeded on sections of their native matrix, they also tend to migrate along the direction of collagen fibril orientation under an aligned EF stimulation.

In addition, 3D studies have revealed that cells behave differently from those in 2D model, both in morphology and protein expression [14, 15]. Cells in 3D studies, such as seeding fibroblasts with in collagen gels, usually lack wide lamellipodias and instead have a more dentric shape, with extended “cylindrical pseudopodia”[16]. These pseudopodia contain both microtubules and f-actin bundles, but the ends of pseudopodia contain mostly f-actin. For protein expression, cells in 3D exhibit a more diffused integrin and vinculin distribution [14], compared to large focal adhesion for 2D flat cells [17]. This diffused attachment may lead to an increase of 3D cell migration, as Sun and coworkers have applied a EF on cells embedded in 3D collagen gels and

demonstrated that compared to cells on glass slides a smaller EF strength is sufficient for 3D cells to migrate [18]. Sun then suggests that in 2D systems, which requires more EF strength, may represent an “exaggerated state of cell adhesion.”

### **3. Hypothesis: Matrix stiffness affects cell migration in aligned collagen matrix**

In this study we apply anterior cruciate ligament fibroblasts (ACLF) to study the differences of 2D and 3D migration. Yet, we also consider the native aligned, tensional environment of ACLFs and hypothesize that their migration may also be affected by tensional homeostasis. Tensional homeostasis is the tendency of cells to regulate cell contractile forces in response to an increase of outside microenvironment tension, for instance, a soft or rigid collagen matrix. Matrix stiffness regulates many cellular activities. For example, cells in 3D collagen gels [17] or on soft substrates lack focal adhesion [19]. Also focal adhesion size and amount are found to decrease when cells are located further from the bottom glass slide and deeper into the 3D gel, thus a softer environment [20]. Matrix stiffness also has a dominant effect on Rho activity. In fact, a soft floating collagen matrix can down regulate Rho even when cells are incubated with serum, which contains growth factors that stimulates Rho activity [21].

This mechanotransduction of Rho and focal adhesion seem to form a feedback

model that affects each other. Focal adhesions act as transducers for sensing matrix stiffness by linking the ECM to the cytoskeleton, and as the stiffness of the ECM increases, cells respond by up regulating Rho, Rock and myosin to increase cell contraction [21], yet up regulation of Rho also increases focal adhesion kinase (FAK) phosphorylation.

The Rho and focal adhesion crosstalk regulation is still not fully understood, but a possible mechanism is through microtubule. Rho regulation shifts the glu/try tubulin ratio [22], resulting in a more stabilized (glu-dominant) or dynamic (try-dominant) microtubule network. This affects integrin turnover rate as microtubule is found heavily involved in focal adhesion disassembly [23] and integrin trafficking [24].

Adding in the factor of matrix thickness, we examined cell migration in aligned collagen matrix with different collagen heights. Aligned collagen were created by combining flow inducing techniques [25] and initial cold incubation [26]. EF is preferred then chemical gradient to serve as a cell migration stimulation, due to its ease of applying a homogeneous field over cells embedded in 3D gels [27]. EF was subjected on cells whether parallel or perpendicular with the original collagen direction, and cell migration speed, angle and directional velocity, a parameter from multiplying cell migration speed and angle, are used to represent overall cell migration inclination. Cell



morphology is observed by examining the two major cytoskeletons: actin and microtubule. Finally, possible underlying mechanisms that effect cell migration are discussed.



# Chapter 2

## Materials and Methods

### 1. Cell Culture

Anterior cruciate ligament fibroblasts (ACLFs) are harvested from porcine knee via matrix digestion. ACL were taken from young porcine ankles and was first cut into cubes of sizes about 5\*5\*5 mm and then wash briefly with a 9% Pluronic® F-68 (Sigma, 10% sterile-filtered) in 1X PBS solution (Biowest) [28]. The explants were then transferred into a centrifuge tube containing sterile 0.2 % type I collagenase (Gibco) in culture medium, which contains DMEM (Biowest), 10% FBS (Sigma), penicillin (100 U/mL, Gibco), and streptomycin(100 U/mL, Gibco). The tube was then kept on a shaker at 37°C for 18hr. After incubation, the mixture was passed through a cell strainer (BD) and then centrifuge at 3000rpm for 10 min. The supernatant was discarded and the cell pellet was re-suspended with culture medium.

ACLFs were seeded in T-75 flasks at 1 million cells per flask and were cultured for 5~7 days before used for further experiments. Culture medium was changed every 3 days.

## **2. Microchannel Fabrication**

Collagen matrix alignment was prepared by sheer stress caused by flowing collagen solution through a polydimethylsiloxane (PDMS) microchannel [25]. Specific dimensions of the PDMS microchannels were fabricated according to soft lithography procedures [29] (figure 1). In brief, SU8 photo resist (Gersteltec Sarl) was spin coated on a silicon wafer, exposed with UV and developed to reveal patterns. The microchannel was designed with dimensions of Height: 400  $\mu\text{m}$ , Width: 3mm, Length: 10mm, and the inlet of the microchannel was branched to increase homogeneity of the injected flow. PDMS (Sylgard 184, Dow Corning) was molded over the SU8 master, and allowed to set for two days before separating the PDMS microchannel from the master, PDMS channels were then cured at 70°C over night.

After cooling down to room temperature, the PDMS channels were punctured and carved for inlets and outlets. As shown in figure 1C, the outlet is funnel shaped in contrast to the inlet. This design maintains the liquid surface level difference between the inlet and the outlet thus induces siphon flow that causes sheer stress.

## **3. Collagen Preparation**

The PDMS microchannel was sterilized with EtOH, air dried in hood, treated with

3% Pluronic<sup>R</sup> F68 overnight to prevent collagen adhesion [30] , rinsed with sterilized water and air dried in hood before use. In order to handle samples more easily, glutaraldehyde treated glass slide were used to increase collagen matrix adhesion [31]. Silane coated glass slides were immersed in 5% of glutaraldehyde (25% Aqueous Solution, Electron Microscopy Science) in 1X PBS for 30 minutes, rinsed with de-ionized water, immersed in EtOH for 30 minutes for sterilization, rinsed with sterilized water and air dried in hood. The PDMS channels were then bonded to the GA treated slides to enclose the channels.

Collagen (BD, rat tail collagen type I) is prepared following suggested protocols of the manufacturer. Namely, 1M NaOH, 10X PBS and purified water were used to neutralize collagen solution, while culture medium was used for dilution, giving a final pH of about 7.4 and a collagen concentration of 3 mg/ml. Collagen solution was then kept at 4°C for 90 minutes before further experiments [26].

After the 4°C cold incubation, four kinds of collagen samples were prepared by combining 2 factors: cell position (2D or 3D) and matrix thickness (thin or thick).

For aligned 3D thin collagen studies, ACLF cell suspensions were trypsinized (Trypsin-EDTA 0.25% , Gibco) from flasks and added to collagen solutions, resulting in a 1.5 g/ml collagen and 200,000 cells/ml mixture. Immediately after mixing, 500 µl

of the collagen mixtures were injected and added on to the inlet of each channels, initiating the siphon flow (figure 2A). For control, random collagen matrices were prepared by spreading 40  $\mu$ l of the mixtures on 1  $\text{cm}^2$ . All collagen samples were incubated for 10 min at 37°C for gelation, and the PDMS channels were then removed as culture medium was added.

For aligned 2D thin or thick collagen studies, 100  $\mu$ m or 400  $\mu$ m microchannels were flooded with collagen solutions that were adjusted with culture medium to 1.5 mg/ml. For control, 40  $\mu$ l of the collagen solution was spread on 1  $\text{cm}^2$ . After gelation, the PDMS channels were removed and ACLFs were seeded on the matrices at 3000 cells/ $\text{cm}^2$ .

Cells mixed in 3D collagen samples tend to sink to the bottom of the collagen gel during gelation, resulting in a thin collagen thickness (figure 3). For comparison, we developed a doubled layered 3D samples to represent a thick 3D collagen sample. These samples (figure 2B) first use a “wall and ceiling” composed 400  $\mu$ m height channel to prepare the first aligned collagen layer without cells, and then uses a 400  $\mu$ m normal channel to add on a second layer of collagen with cells.

All collagen samples were incubated for 24 hr without changing culture medium before being used for further cell migration studies.

#### **4. Pharmacological reagents**

Rho-kinase (ROCK) of ACLFs were inhibited with Y27643 that was dissolved as 20mg/ml in DMSO (sigma) as stock solution. After samples were prepared, cells were incubated for 24 hr, and then were treated with a final concentration of 10 $\mu$ M of Y27632 (Caymen) in medium for 4 hrs [32]. Samples were then rinsed with fresh culture medium before further migration studies.

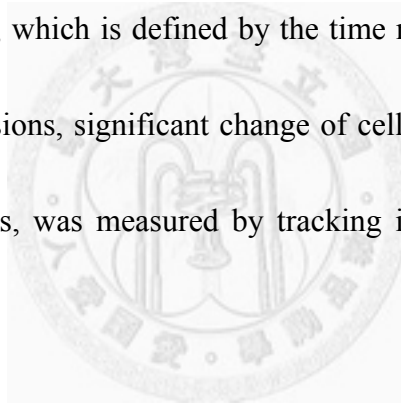
#### **5. Electric Field Studies**

The 3D cell cultures are subjected to applied DC EFs in a modified electrical stimulation chamber and placed on an inverted microscope, as shown in figure 4 [33]. Two EF applying methods are used, parallel or perpendicular to the aligned collagen direction. Images are taken every 15 minutes for 2 hours. Each experiment is repeated at least three times.

#### **6. Cell Morphology and Migration Analysis**

Cell spreading area, orientation and migration was measured in this study. Cell spreading area was measured by circling cells using the “free hand selection” of image J. Cell orientation was measured by the angle between the EF axis and the long axis of the

oval that best circles the cell. For cell migration, it has been shown that fibroblast migration in 3D collagen matrix under EF can be characterized by assuming “planar lateral cell migration [18].” In other words, fibroblasts migrate mostly in the plane of observation, and movement in the optical axis can be neglect. Therefore, cell migration speed and angle ( $\theta$ ) along the EF axis is calculated by the displacement of the geometry centroid of each cell. Directional velocity, a representation of cell migration in the direction of the field, is calculated by multiplying migration speed with  $\text{Cos}(\theta)$ . Cellular tail retraction time, which is defined by the time needed for cells to perform a sudden retraction of protrusions, significant change of cell spreading area and increase of cell migration afterwards, was measured by tracking individual cells along an EF study time course.



## **7. Scanning Electrical Microscopy**

Collagen samples were fixed with 0.5% GA for 30 minutes, stained with 0.5% Osmium tetroxide (Electron microscopy science) for 30 minutes followed with graded series acetone dehydration. Collagen samples were then substituted into t-butyl alcohol (Sigma) and then freeze dried overnight [34]. The dried samples were mounted on an aluminum stub, coated with gold using a sputter coater, and observed with a field

emission SEM.

## **8. Immunofluorescence Microscopy**

Cells were stained according to protocols from previous works with modifications [16]. Cells were fixed with 3% formalin in 1X PBS for 1 hr, washed 3 times with PBS, permeabilized with 0.5% Triton X-100 (Sigma) in PBS for 30 min and then washed 10 min each for 3 times with PBS. Cells were then blocked with a mixture of 5% horse serum (SAFC) and 0.05% TWEEN(Sigma) in 1X PBS (HTPBS) for 30 minutes, and then treated with primary antibodies (anti  $\alpha$ -Tubulin, clone DM1A, Sigma) in HTPBS at 4°C overnight. Afterwards, cells are washed 10 min each for 3 times with HTPBS, and then treated with secondary antibodies (Alexa Fluor® 568 goat anti-mouse IgG, Molecular Probes) at 1:200 in HTPBS for 4°C overnight. Cells were then washed with PBS alone. To stain F-actin, phalloidin (Alexa 488-conjugated phalloidin, Molecular Probes) was used for 30 minutes after the immunostaining.

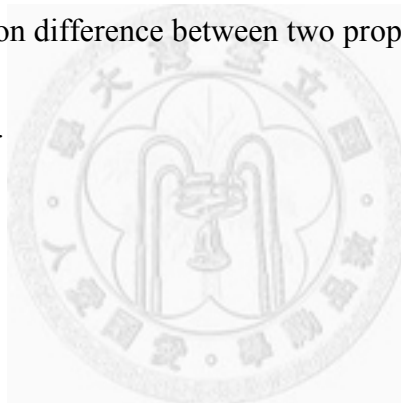
Cells were visualized with either a 40X or 60X water immerse objective on a Leica TCS SP2 confocal microscopy. Collagen fibrils are also visualized with the reflectance mode as in previous literature [35]. Namely, using a 488nm laser for excitation and imaging with a band pass filter of 490~500 nm. Co-localization analysis of actin and tubulin was performed by analyzing image stacks with an image J plugin



“Intensity correlation analysis” [36]. Collagen orientation was measured by applying a “Fourier transform” function in Image J and then using the “Oral profile” function to sum up the spectrum area in each degree [37].

## **9. Statistical analysis**

STATISTICA (Statsoft) was used to perform Student’s t-test and ANOVA analysis with post-hoc tests (LSD,  $\alpha=0.05$ ). P-value of cell detachment percentage was calculated by pair comparison difference between two proportions, and then multiplying p with the total pair number.



## Chapter 3

### Results

Collagen fibril formation is shown to be affected by multiply factors: incubation temperature, electrolyte concentration and pH. To confirm the collagen morphology of our samples, SEM was used to examine the collagen structure. Figure 5 shows the morphology of collagen fibrils using whether 130 mM NaCl (Fig 5A) or DMEM (Fig 5B) as diluting solution. The fibrils in DMEM show bundle like structures, in contrast to thin, network like fibrils in 130mM NaCl.

Collagen fibrils can be aligned by sheer flow deposit. Figure 6A and 6B compares sheer flow aligned collagen with random collagen. Despite having cells embedded in them, collagen fibrils in flow induced samples show alignment. Therefore this indicates that the inlet flow is not disturbed even when cells are included in the collagen mixture. Saeidi and coworkers have suggested a model for computing the sheer stress on the floor of microchannels by approximating the system as a 2-dimensional flow between two flat plates [25]. By assuming laminar flow, which gives a no-slip condition on the glass, the shear stress on the floor can be computed as:

$$\tau = \frac{6\mu Q}{wH^2}$$

Where  $\tau$  is the shear stress on the floor,  $\mu$  is the dynamic viscosity of the solvent,  $Q$  is the flow rate,  $w$  is the width and  $H$  is the height of the microchannel. In addition, the flow rate can be calculated by Bernoulli's equation. By assuming zero flow speed at the reservoir and zero elevation at the channel, we can compute that:

$$Q = wH\sqrt{2gz}$$

With  $g$  is the acceleration due to gravity and  $z$  is the elevation of the reservoir. By substituting  $Q$  we can find shear stress  $\tau$  as:

$$\tau = \frac{6\mu\sqrt{2gz}}{H}$$

As shown in this equation, shear stress is proportional to the square of reservoir elevation when the channel height is fixed. In our experiment, we used a PDMS with 400  $\mu\text{m}$  channel height and changed the inlet reservoir height by 4mm, 8mm and 12 mm. As shown in figure 6C, the alignment of collagen fibrils to the x axis increases from random to 4mm to 8 mm. For the 8mm groups, the percentage of fibrils lying between  $\pm 15$  degrees is significantly higher than other groups (Fig 6D). Therefore, 8mm was set for inlet height for future experiments. The decrease of alignment for 12 mm groups may result from higher flow rates, which drains the reservoir too soon before collagen gelation. Collagen fibrils in double layer samples are also examined. Collagen fibrils that are 50  $\mu\text{m}$  above the interface (between the first and second layer) still shows

significant alignment, compared to those in random collagen. This indicates that fabricating multiple layers of aligned collagen is possible.

Cells align to the aligned matrix, whether in 2D or 3D samples. Figure 7A and 7B shows cell orientation distribution of 3D and 2D samples. Cell orientation is defined by the major axis of the oval that best circles the cell. In parallel collagen samples, both 2D and 3D cells show alignment along the x axis, while cells in random collagen do not. Figure 7C shows that in parallel collagen samples, over 50% of cells lie in  $\pm 15$  degrees to the x axis, which is significantly more than random samples.

By examining cross sectional view, we found that during collagen gelation, cell in 3D samples mostly sink to the bottom of the gel, a position similar to 2D thin samples (figure 3). In contrast, cells seeded on 2D thick or embedded in 3D thick collagen matrix are found 100  $\mu\text{m}$  above the glass slide.

The thickness of collagen gel affects cell morphology. As shown in figure 3, both 2D thin and 3D thin cells express stress fibers that are aligned to the collagen orientation. In contrast, cells in the 2D thick and 3D thick samples do not express stress fibers, and are localized in the distal ends of pseudopodia. The degree of actin and tubulin colocaliation is also significantly higher in thin aligned collagen samples. The average Pearson correlation coefficient for thin samples is 0.6, in contrast, thick

collagen samples are around 0.35. However, no significant difference was found between 2D random and 3D random, even they have similar collagen gel heights with aligned samples.

Cell migration in 3D and 2D collagen matrix seem to divide into two phases: tail detachment and persistent migration. This phenomenon is illustrated in figure 8A. At the beginning of EF stimulation, cells in aligned collagen samples show a bipolar shape due to contact guidance of collagen fibrils. As EF stimulation begins, cells express increase activity of protrusions on the side facing the cathode. However, cells need to retract protrusions on the rear side, to then significantly migrate toward the cathode. Figure 8B shows the percentage of cells that undergo a detach phase, and indicate that cells in soft aligned samples (2D thick and 3D thick) significantly detach more easily than others cells. In addition, cells that are parallel to the EF show a trend of a higher detach percentage then perpendicular cells of the same condition. We also examined whether actin and tubulin co-localize in a cell, but did not found any trend. Notably, 2D thick parallel cells have a high detach rate and a low actin/tubulin co-localization degree.

Contact guidance is more dominant then EF stimulation. Figure 8C shows polar plots of cell under EF stimulation. In general, cells tend to migrate in both ways along

the collagen fibril direction, with preference toward the cathode side in 3D thin samples and the anode side in 3D thick samples. Cells in 3D random collagen matrix show a more scattered migration pattern, as 2D random samples express tendency toward the cathode.

Matrix thickness affects cell migration directionality but not migration speed. In figure 9 shows cell directional velocity towards the cathode (figure9A) and cell migration speed (figure 9B). In general, cell migration speed is increased about two fold under EF stimulation, but there is neither significant difference from matrix thickness, nor from 2D or 3D conditions. However, these two factors affect directional velocity. In 2D thick random samples, cells show significant migration tendency toward the cathode compared to cells without EF. Also, cells in 3D thin aligned collagen matrix show significance when the EF axis matches the collagen orientation.

Inhibiting Rho-kinase (ROCK) increases cell migration directionality. ROCK is a downstream factor of Rho and is found to regulate actin formation and myosin II, thus, increases cell contractility. By inhibiting ROCK, 2D cells all show dominant directionality toward the cathode, whether random or aligned, thin or thick, (figure 10A). Also, 3D cells show a change of migration tendency toward the cathode, especially as 3D thick aligned cells show a change from anode to cathode. However, 3D cells'

directionality is not as dominant as 2D cells. This difference between 2D and 3D probably results from the effect of ROCK inhibition on migration speed. For example, aligned 2D cells show no increase in migration speed, yet all 3D samples show a decrease in migration speed (figure 10B).



## Chapter 4

### Discussion

In this study, we have developed a model to examine cell migration in an aligned collagen matrix, combining the influence of matrix stiffness. Collagen fibrils are significantly aligned in our system, disregarding the different heights and cell positions. Many methods have been proposed to align collagen fibrils, such as applying electro-spinning [38], magnetic [39], dip-pen nanolithography [40] and freezing and thawing [41]. Above all, these approaches require complicated methods and systems to achieve the goal. Although our method may not exceed other methods in collagen alignment degree, the ease of preparing and the possibility of designing specific flow pattern and matrix thickness allows us to create different microenvironments to meet experimental needs.

ACLFs show contact guidance and alignment in an aligned collagen matrix, this phenomenon is found whether in 2D or 3D, thin or thick samples. It is possible that cells' contraction during incubation causes the gel to align more, as the tension is transmitted throughout the gel and collagen gel is known to align between cells [42]. Since the collagen is fixed to the glass slide surface through GA, the collagen gels can be viewed as a fixed fibroblast populated lattice model (FPLC), where cells develop



tension in contrast to non-fixed floating gels. Although many studies use the FPLC model as a 3D representative [43], our findings that cells tend to sink to within 50 $\mu$ m from the glass surface suggest that future studies should take this aspect in consideration. Cells that end up at the surface between the gel and glass slide, may form attachments with the glass slide, and therefore show significant morphology differences from cells that are totally embedded in the gel [17].

By examining cell migration in collagen samples, we found that cells exhibit a two phase migration pattern: protrusion detachment and migration. The percentage of detachment is related with EF stimulation orientation and matrix stiffness. While EF is known to cause cell polarization, it is possible that cells that are parallel to the EF are more polarized than cells that are perpendicular, since the cell is subjected with a higher total voltage drop. Also, matrix stiffness may be related with protrusion detachment, possibly through glu-microtubule regulation. Matrix stiffness has been shown to relate with Rho activity, as a soft matrix can down-regulate Rho activity, even with serum stimulation [21]. In addition, enhancing Rho is shown to up regulate glu-tubulin, while inhibiting Rho disrupts this structure [22]. Since microtubule has been shown to target, reach and disassemble focal adhesion [44], a upregulation of glu-tubulin may deter cell's ability to disassemble focal adhesions. In fact, stabilizing microtubule with taxol does

inhibits this phenomenon [44]. The up regulation of  $\alpha$ -tubulin is not related with actin stress fiber [23], and indicates that a stiffer microtubule network is directly regulated when cells are subjected to higher tension states.

Basing on cell migration polar plots, we found that cells under EF stimulation seem to prefer to follow contact guidance in all groups. This finding matches with other studies [12] and our previous work of cell migration on ligament sections. In addition, we found that although cells do prefer to migrate along collagen fibrils, the mechanotransduction of matrix stiffness is also incorporated in the process. For example, 3D cells in soft aligned collagen gels express an anode-side directionality, in contrast, 3D cells in thin aligned collagen gels show cathode-side migration tendency.

By inhibiting ROCK with Y27632, cells in 3D samples show a decrease in cell migration speed, compared to 2D samples which mostly do not. This might be explained that cells might require more strength to infiltrate a 3D collagen network, compared to crossing a 2D collagen surface. However, inhibiting ROCK seems to increase directionality in almost both 2D and 3D samples. While Y27632 has little effect on electrotaxis of cells seeded on flat quartz with nanogroves [12], cells seeded on 2D thin aligned collagen gels express an increase in directionality, implying that different integrin attachment are involved. In fact, Y27632 enhances the spreading and motility of FAK-/-

cells [45].

This phenomenon may be explained that cells tend to maintain tensional homeostasis under EF stimulation. When cells are seeded on glass slides are polarized by an EF, a increase of protrusion activity is found on the cathode side [46], and cells extend protrusions perpendicular to the EF axis. A possible reason is that cells sense the stiff glass slide surface and try to re-establish a high-tension state, yet as the front side of the cell is constantly ruffling under EF stimulation, therefore cells are forced to change their orientation, develop stress fibers and contraction forces perpendicular to the EF axis [47].

Considering this effect in our study, cells on a 2D aligned matrix sense the anisotropic collagen fibrils and try to re-establish a new tension balance with the outside environment under EF. However, the matrix mainly provides support along the fibril. Also, contact guidance suppresses cells ability to form new attachment across fibrils. As a result, cells are stuck in desperate state trying to maintain tensional homeostasis, causing the cells to migrate in both direction along the fibrils. In contrast, cells on a 2D random collagen gel supposing are in a more low tension state, therefore cells can show high directionality under EF stimulation.

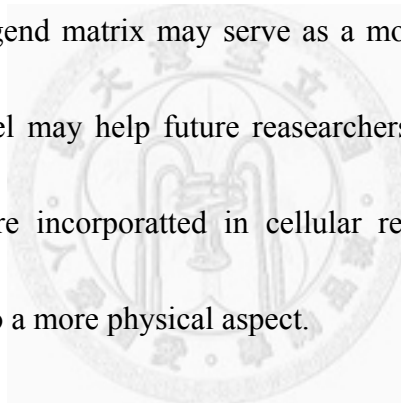
This aspect may also explain the high directionality of 3D thin aligned cells, as

fibrils near the glass slide are fixed and therefore provide more side support. However, directionality is not the case in 2D thin aligned samples. One possible reason is that 3D cells, although still in a stiff microenvironment, still express weaker focal adhesion than 2D cells. This is supported by when in thin collagen samples, 3D cells still have a higher detachment rate than 2D cells. Another possible reason is that cells in 3D are allowed with more attachment around the cell body, in contrast to the limitation of the base surface attachment of 2D cells. 3D cells are likely to have more side support than 2D cells, and therefore are more able to balance forces along the EF stimulation and profit from contact guidance to increase directional migration.

By treating cells with ROCK inhibitor Y27632 prohibits cellular actin filaments formation and cell contractility [45]. However, Y27632 does not disrupt zyxin-containing adhesion structures at the cell periphery and leading edge [48]. This means that inhibiting ROCK only deters cellular tension state, not cellular attachment. In our study, ROCK inhibited cells show increasing directionality under EF, without a significant increase in migration speed. This may indicate that ROCK inhibited cells are prevented to maintain tensional balance with the outside environment, therefore showing obedience to the EF stimulation.

In conclusion, we have developed a microfluidic method of aligning collagen

fibrils. This method allows us to examine cell behavior and cell migration in different gel thickness and conditions. We found that despite cells tend to follow contact guidance under EF stimulation, the directionality of cells varies from dimensional conditions and matrix stiffness. This may indicate that traditional cell studies on 2D glass slides, which cells are flattened and tensioned, may not be able to fully represent cellular behavior in their in vivo conditions. As more and more studies demonstrate that a physical [9, 49] or spatial stimulation [50] can dramatically change cell morphology, gene expression and behavior, our model of aligned matrix may serve as a more closer analogy to in vivo conditions. Thus our model may help future researchers to understand how tension and dimensionality cues are incorporated in cellular regulation, and discover new cellular mechanism related to a more physical aspect.



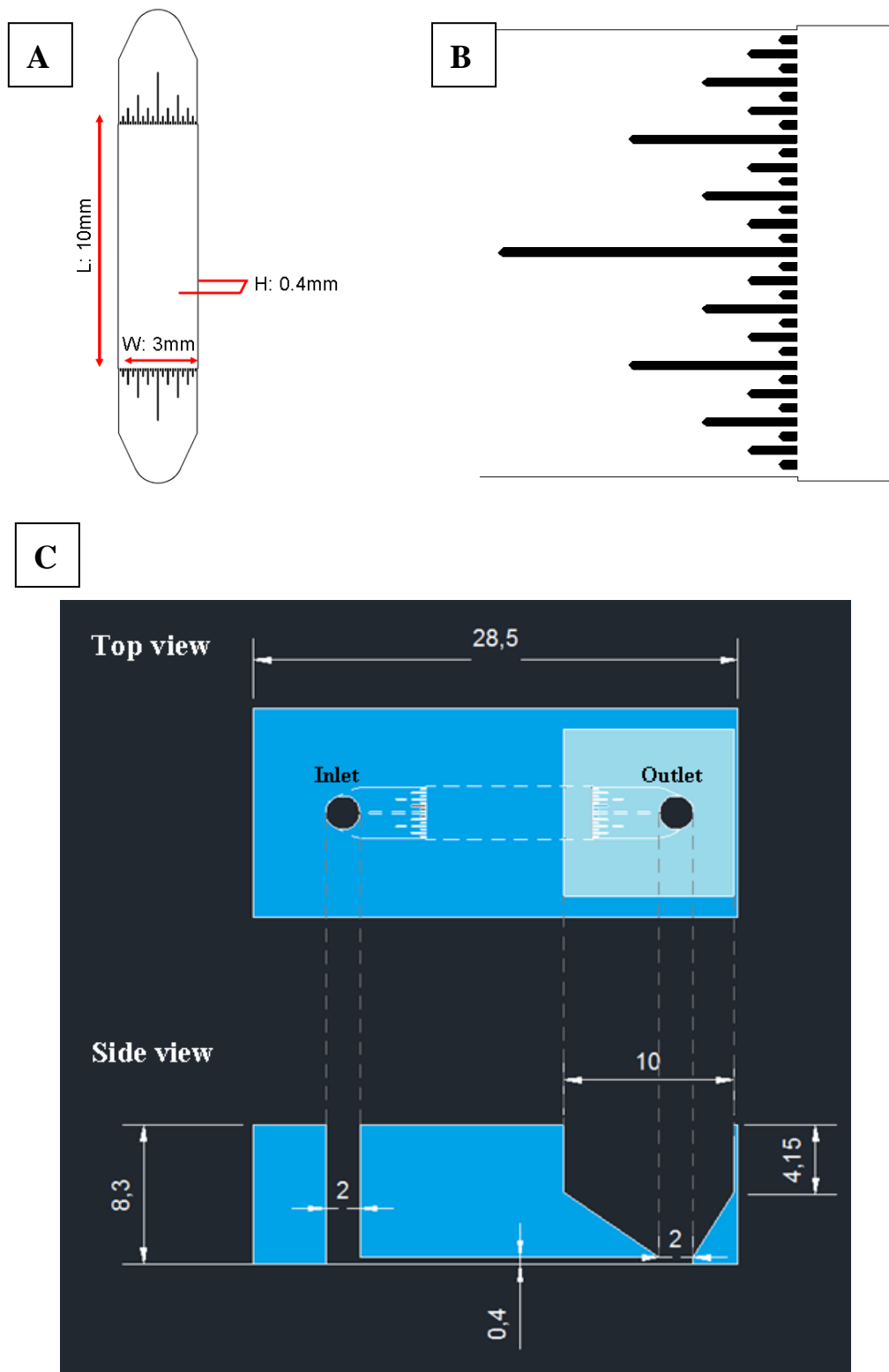


Figure 1. Pattern of microchannel. (A) Dimension of the main channel. (B) Bifurcation at the inlets of the main channel. (C) Dimensions of PDMS microchannel. Unit: mm.

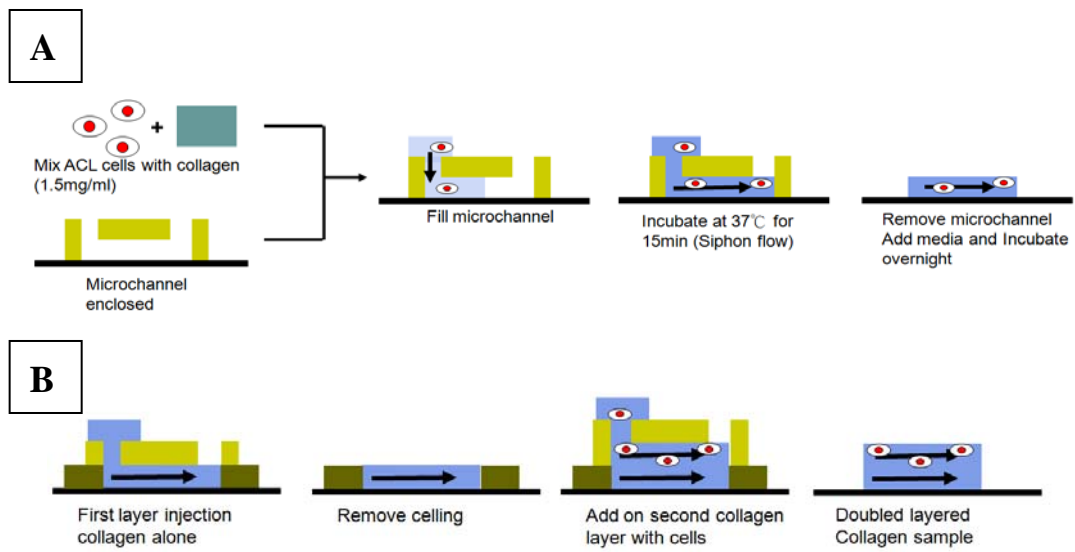


Figure 2. (A) Procedure of preparing 3D aligned collagen samples. (B) Procedures of preparing a doubled layer 3D sample.



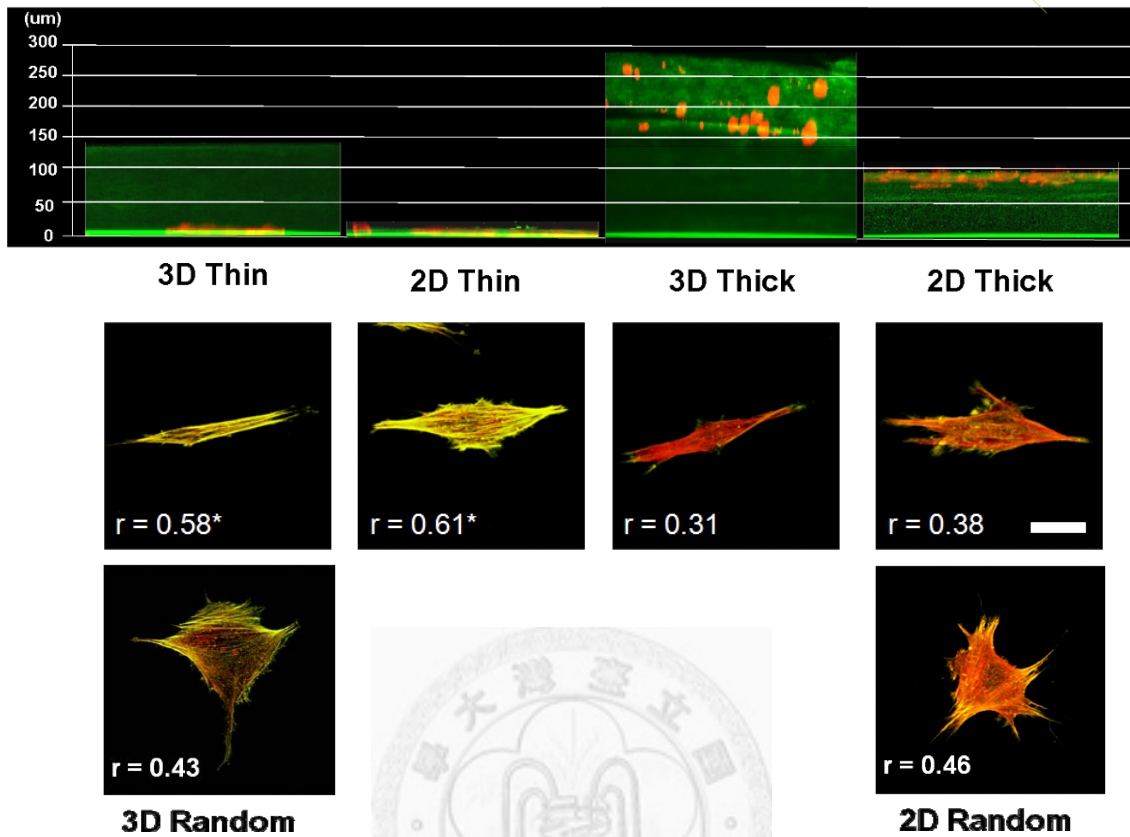


Figure 3. Above: Cross-sectional image of different collagen samples. The bright green layer at the bottom of each picture is caused by reflection of the glass slide surface. Red: Actin. Green: Collagen. Below: Cell morphology after 24hr corresponding with different collagen gel heights. Cells are stained for  $\alpha$ -tubulin (Red) and F-actin (Green), yellow is shown when the two co-localize. R value: Pearson correlation coefficient of actin and tubulin. Statistical significance: (\*)  $p < 0.05$  against thick aligned samples. N=3 for each group. Scale bar: 40  $\mu$ m.



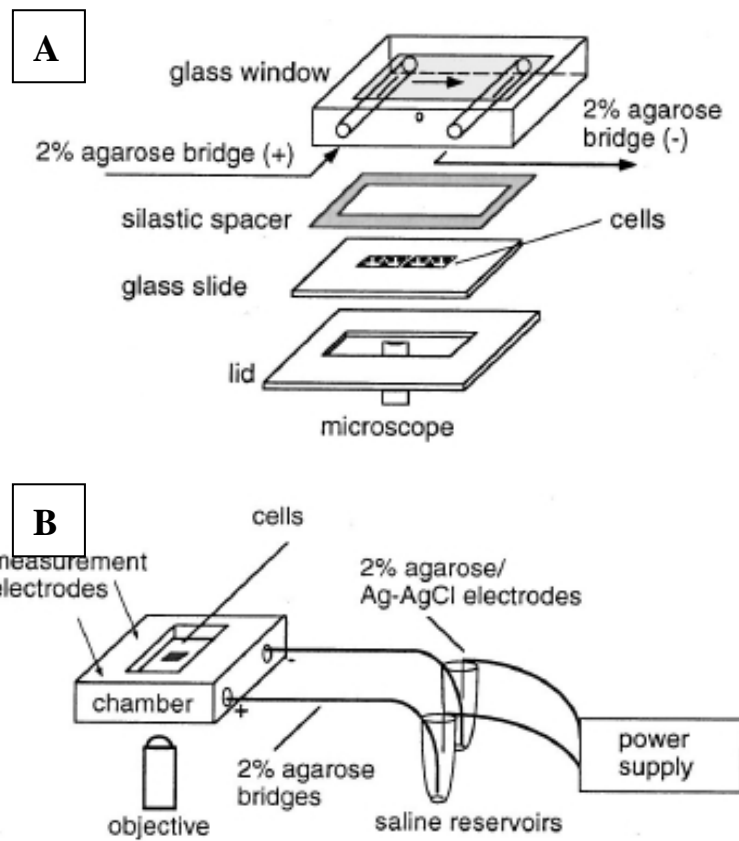


Figure 4. Electrical stimulation chamber. (A) Components of the chamber. (B) The chamber is connected to saline reservoirs with 2% agarose salt bridge and electrical current is applied with a power supply.

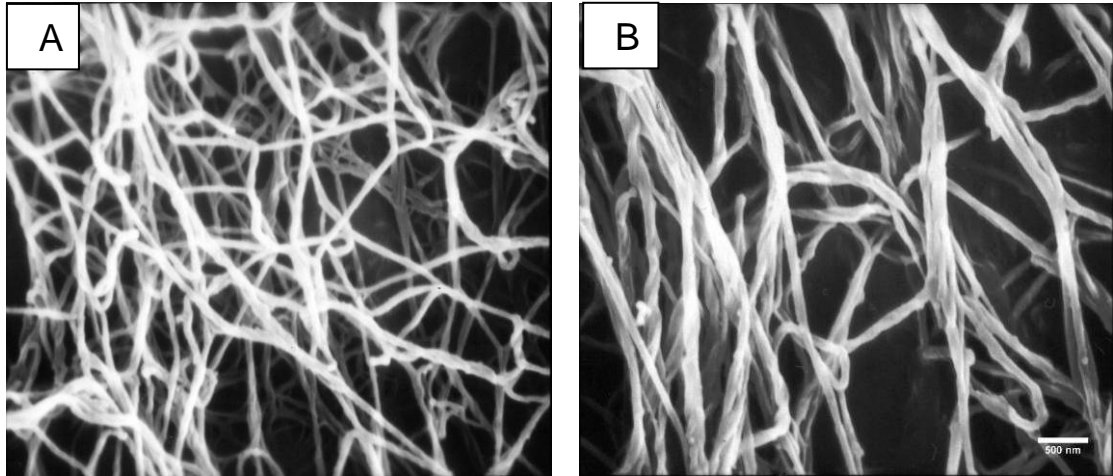


Figure 5. SEM of collagen fibril with incubated at 4°C for 90 min after pH neutralization, (A) diluted with 130mM NaCl (B) diluted with DMEM. Scale bar=500nm



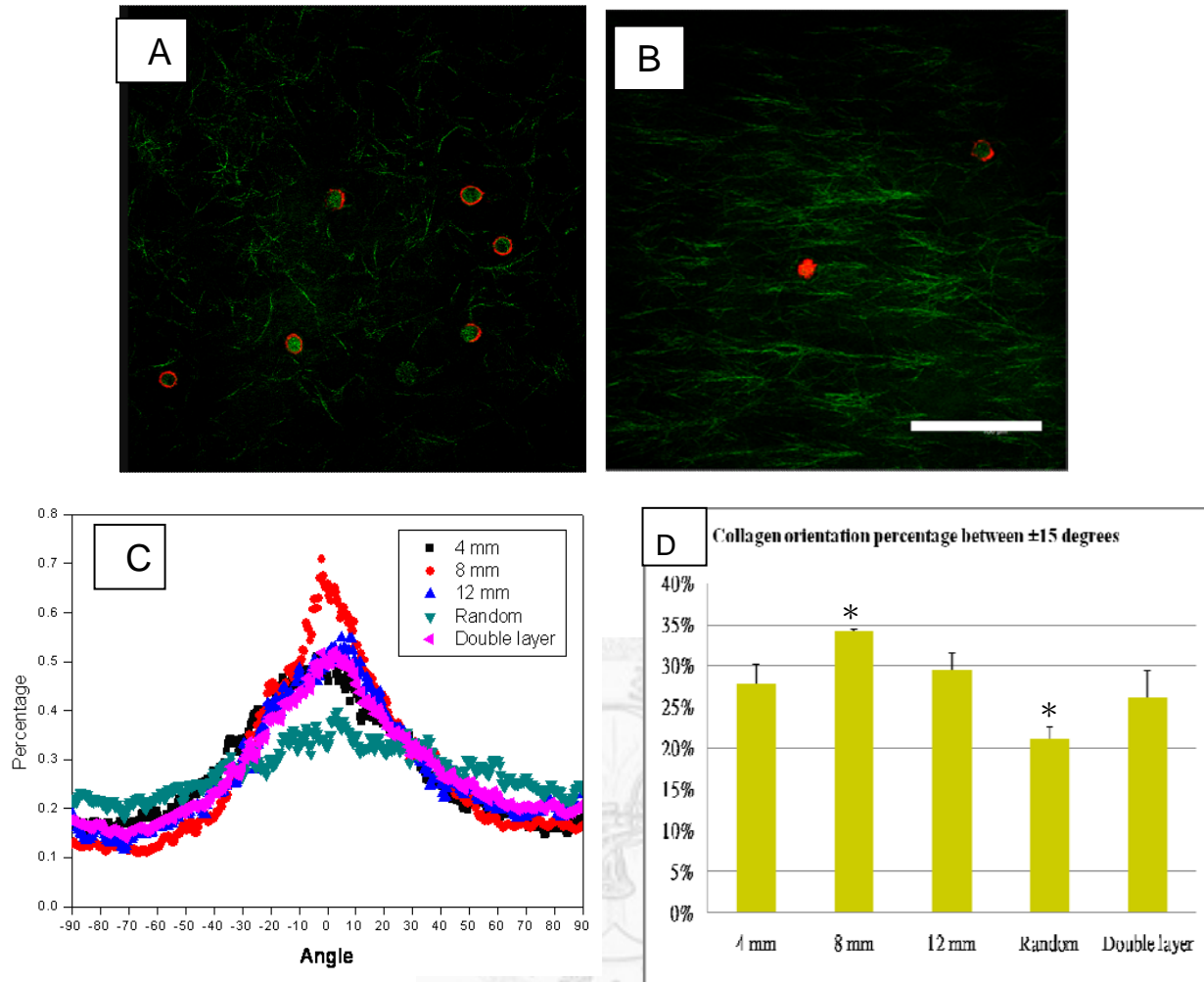


Figure 6. (A) ACLF in random collagen and (B) aligned collagen. Cells are fixed and stained for actin (Red) after collagen gelation (Green). Scale bar=100  $\mu$ m. (C) Collagen fibril angle distribution. Flow induced collagen within PDMS channels with 4mm, 8mm and 12 mm inlet heights are compared to random collagen gel and doubled layer collagen samples. (D) Total percentage of collagen fibril angle within  $\pm 15$  degrees. Statistic significance: (\*)  $p < 0.05$  against all other groups. N=3 for each group.

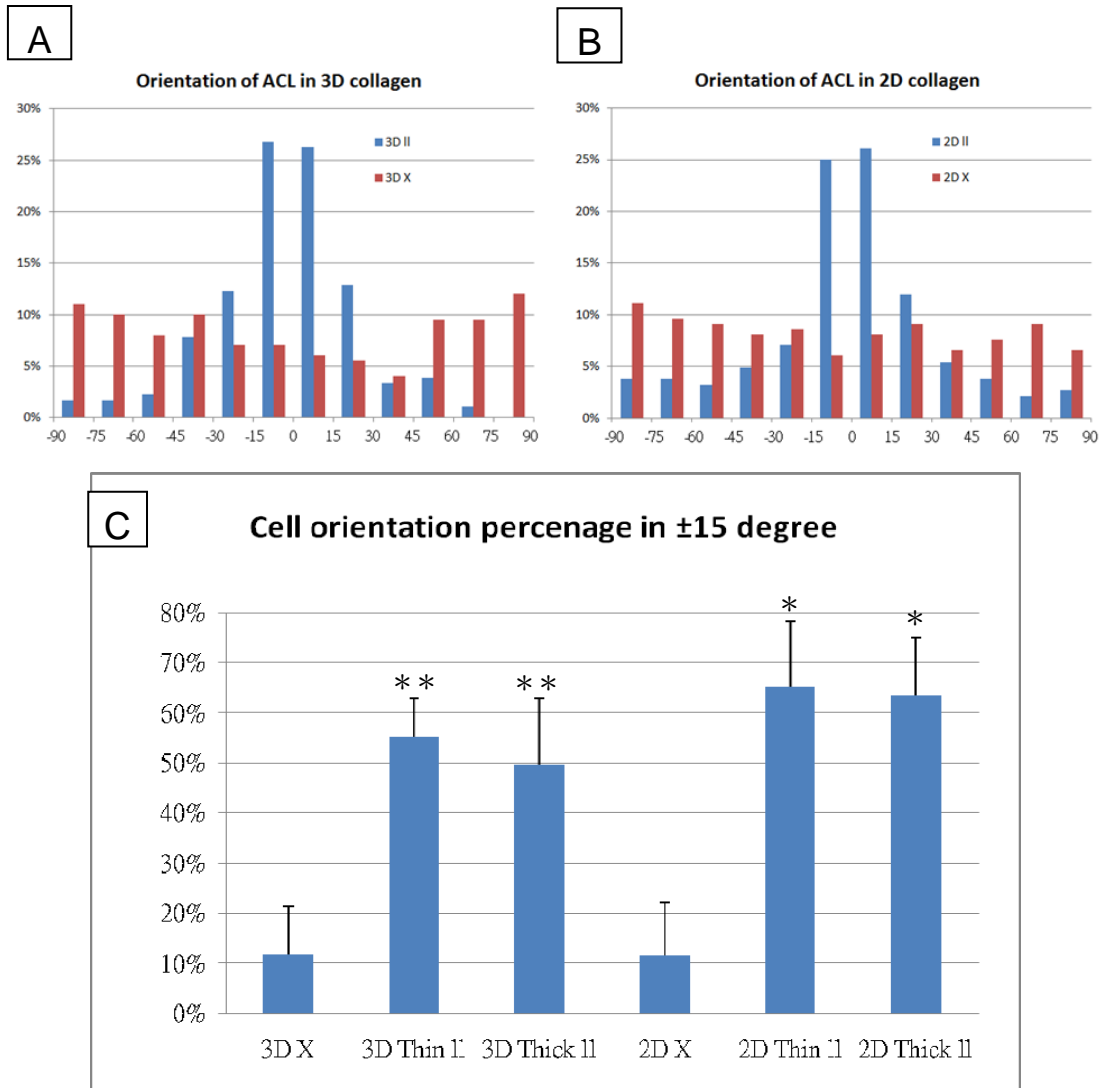


Figure 7. Cell orientation distribution in (A) 3D collagen samples and (B) 2D collagen samples. Symbol representative: (II) parallel (X) random. (C) Cell total cell orientation percentage within  $\pm 10$  degrees. Statistic significance:  $p < 0.05$  for (\*) against 2D random and (\*\*) against 3D random.  $N=6$  for each group.

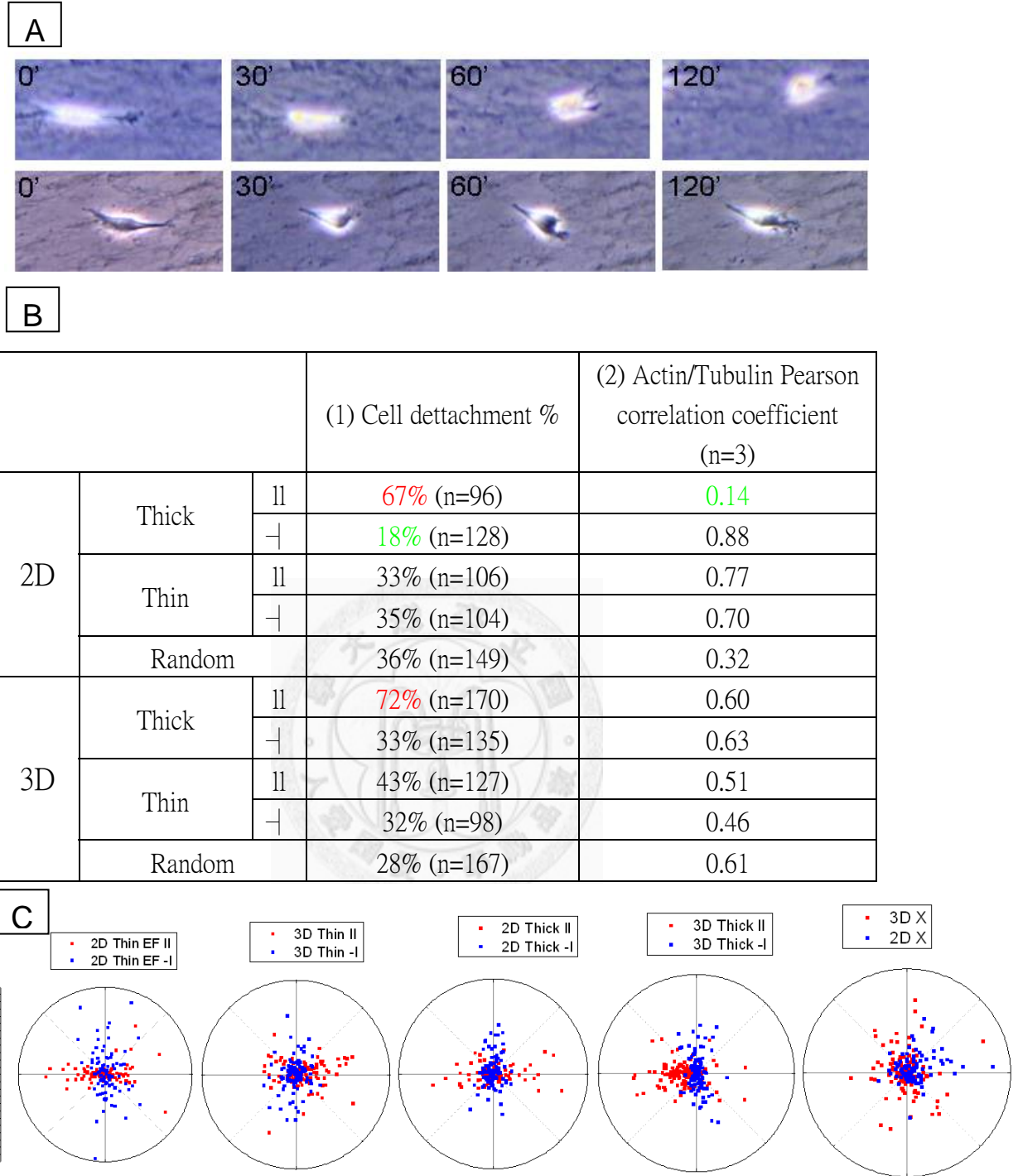


Figure 8. (A) Examples of cell migration under EF stimulation. Tail retraction is required for cells to migrate. Upper: 2D aligned thick. Lower: 2D aligned thin. (B) Table of (1) Percentage of cells that undergo detach during a 2 hr EF study (2) Pearson correlation coefficient of actin and tubulin co-localization. Symbol representative: (||) parallel (⊥) perpendicular and (X) random. Statistic significance:  $p < 0.05$  for red (higher) and green (lower) then figures in black. (C) Polar charts of cells under EF stimulation, cathode at right hand side.

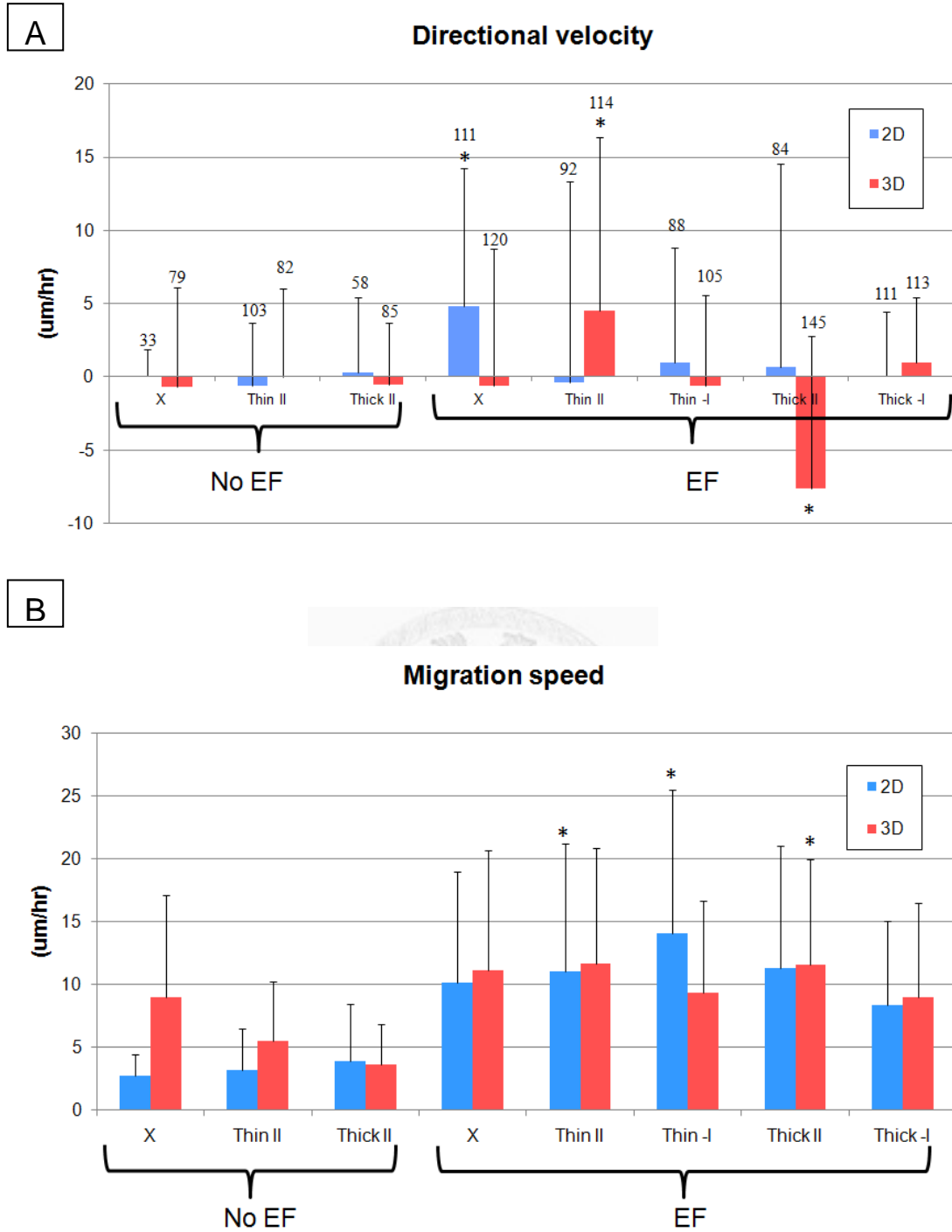


Figure 9. (A) Directional velocity of ACLF toward cathode. Number above error bar denotes sample number. (B) Migration speed of ACLF. Symbol representative: (II) parallel (-I) perpendicular and (X) random. Statistic significance:  $p < 0.05$  for (\*) against all no EF groups.

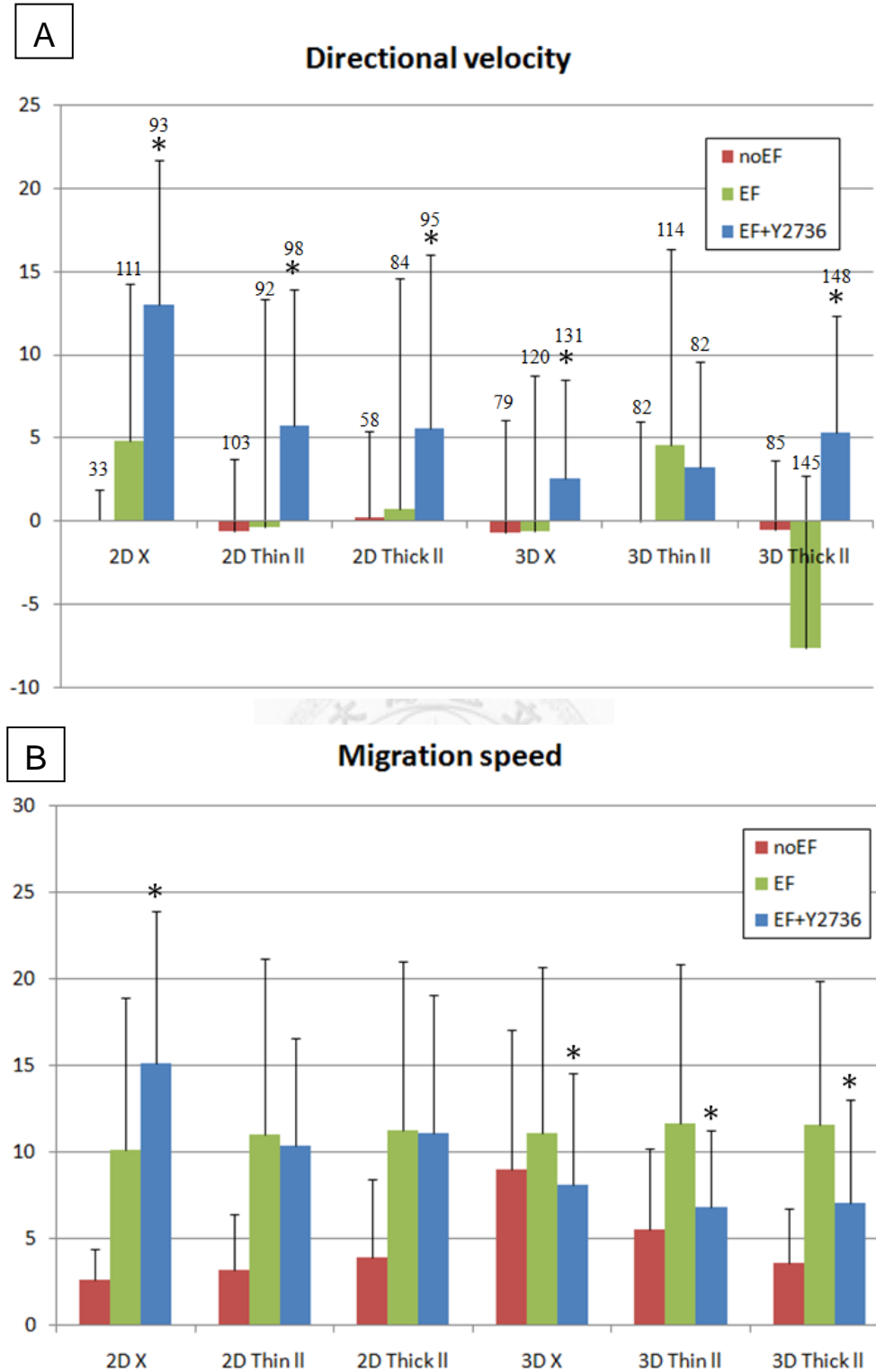


Figure 10. Comparison of Y2736 treated (ROCK inhibition) cell migration (A) Directional velocity of ACLF toward cathode. Number above error bar denotes sample number. (B) Migration speed of ACLF. Symbol representative: (II) parallel (-I) perpendicular and (X) random. Statistic significance:  $p < 0.05$  for (\*) against each EF groups without drugs of the same collagen gel condition .

## Reference

1. Ridley, A.J., *Cell Migration: Integrating Signals from Front to Back*. Science, 2003. **302**(5651): p. 1704-1709.
2. O. C. Rodriguez, A.W.S., C. A.Mandato, P. Forscher, W. M. Bement, C. M. Waterman-Storer, *Conserved microtubule–actin interactions in cell movement and morphogenesis*. Nature Cell Biology, 2003. **5**(7): p. 599-609.
3. Worthylake, R.A., *RhoA is required for monocyte tail retraction during transendothelial migration*. The Journal of Cell Biology, 2001. **154**(1): p. 147-160.
4. M. D. Welch and M.R. Dyche, *Cellular control of actin nucleation*. Annual Review of Cell and Developmental Biology, 2002. **18**(1): p. 247-288.
5. Emsley, J., et al., *Structural Basis of Collagen Recognition by Integrin  $\alpha 2\beta 1$* . Cell, 2000. **101**(1): p. 47-56.
6. R. Zaidel-Bar, M.C., L. Addadi, B. Geiger, *Hierarchical assembly of cell matrix adhesion complexes*. Biochemical Society Transactions 2004. **32**(3).
7. Yeh, C.-H., C.-H. Chen, and Y.-C. Lin, *Use of a gradient-generating microfluidic device to rapidly determine a suitable glucose concentration for cell viability test*. Microfluidics and Nanofluidics, 2010. **10**(5): p. 1011-1018.
8. Daniel St Johnston, C.N.-V., *The Origin of Pattern and Polarity in the Drosophila Embryo*. Cell, 1992. **68**: p. 201-219.
9. McCaig, C.D., B. Song, and A.M. Rajnicek, *Electrical dimensions in cell science*. Journal of Cell Science, 2009. **122**(23): p. 4267-4276.
10. Chao, P.-H.G., et al., *Effects of Applied DC Electric Field on Ligament Fibroblast Migration and Wound Healing*. Connective Tissue Research, 2007. **48**(4): p. 188-197.
11. Franchi, M., et al., *Tendon and ligament fibrillar crimps give rise to left-handed helices of collagen fibrils in both planar and helical crimps*. Journal of Anatomy, 2010. **216**(3): p. 301-309.
12. Rajnicek, A.M., L.E. Foubister, and C.D. McCaig, *Prioritising guidance cues: Directional migration induced by substratum*



- contours and electrical gradients is controlled by a rho/cdc42 switch.* Developmental Biology, 2007. **312**(1): p. 448-460.
13. Doyle, A.D., et al., *One-dimensional topography underlies three-dimensional fibrillar cell migration.* The Journal of Cell Biology, 2009. **184**(4): p. 481-490.
  14. Grinnell, F., *Fibroblast biology in three-dimensional collagen matrices.* Trends in Cell Biology, 2003. **13**(5): p. 264-269.
  15. Cukierman, E., *Taking Cell-Matrix Adhesions to the Third Dimension.* Science, 2001. **294**(5547): p. 1708-1712.
  16. Martins, G.G. and J. Kolega, *Endothelial cell protrusion and migration in three-dimensional collagen matrices.* Cell Motility and the Cytoskeleton, 2006. **63**(2): p. 101-115.
  17. S. I. Fraley, et al., *A distinctive role for focal adhesion proteins in three-dimensional cell motility.* Nature Cell Biology, 2010. **12**(6): p. 598-604.
  18. Shan Sun, J.W., Michael Cho, *Human Fibroblast Migration in Three-Dimensional Collagen Gel in Response to Noninvasive Electrical Stimulus. I. Characterization of Induced Three-Dimensional Cell Movement.* Tissue Engineering Part A, 2004. **10**(9): p. 1548-1557.
  19. R. J. Pelham. JR, Y.L.W., *Cell locomotion and focal adhesions are regulated by substrate flexibility.* Proc. Natl. Acad. Sci. USA, 1997. **94**: p. 13661–13665.
  20. Fraley, S.I., et al., *Reply: reducing background fluorescence reveals adhesions in 3D matrices.* Nature Cell Biology, 2011. **13**(1): p. 5-7.
  21. Wozniak, M.A., *ROCK-generated contractility regulates breast epithelial cell differentiation in response to the physical properties of a three-dimensional collagen matrix.* The Journal of Cell Biology, 2003. **163**(3): p. 583-595.
  22. Tiffani A. Cook, T.N., and Gregg G. Gundersen, *Rho Guanosine Triphosphatase Mediates the Selective Stabilization of Microtubules Induced by Lysophosphatidic Acid.* The Journal of Cell Biology, 1998. **141**(1): p. 175-185.
  23. Ezratty, E.J., M.A. Partridge, and G.G. Gundersen, *Microtubule-induced focal adhesion disassembly is mediated by dynamin and focal adhesion kinase.* Nature Cell Biology, 2005. **7**(6): p. 581-590.

24. Akhmanova, A., S.J. Stehbins, and A.S. Yap, *Touch, Grasp, Deliver and Control: Functional Cross-Talk Between Microtubules and Cell Adhesions*. Traffic, 2009. **10**(3): p. 268-274.
25. N. Saeidi, E. A.Sander, and J. W.Ruberti, *Dynamic shear-influenced collagen self-assembly*. Biomaterials, 2009. **30**(34): p. 6581-6592.
26. K.E.Sung, et al., *Control of 3-dimensional collagen matrix polymerization for reproducible human mammary fibroblast cell culture in microfluidic devices*. Biomaterials, 2009. **30**(27): p. 4833-4841.
27. al., B.S.e., *Application of direct current electric fields to cells and tissues in vitro and modulation of wound electric field in vivo*. Nature Protocols, 2007. **2**(6): p. 1479-1489.
28. George T. Rodeheaver, L.K., Barbara J. Kircher, Richard E Edlich, , *Pluronic F-68": A Promising New Skin Wound Cleanser*. Ann Emerg Med, 1980. **9**(11): p. 572-576.
29. Sarl, G., *SU8-Photoepoxy GM 1070 Datasheet*. 2005.
30. M. H. Wu, et al., *Development of PDMS microbioreactor with well-defined and homogenous culture environment for chondrocyte 3-D culture*. Biomedical Microdevices, 2006. **8**(4): p. 331-340.
31. Tan, W. and T.A. Desai, *Layer-by-layer microfluidics for biomimetic three-dimensional structures*. Biomaterials, 2004. **25**(7-8): p. 1355-1364.
32. A. M. Rajnicek, L. E. Foubister, and C. D. McCaig, *Alignment of corneal and lens epithelial cells by co-operative effects of substratum topography and DC electric fields*. Biomaterials, 2008. **29**(13): p. 2082-2095.
33. P.G.H. Chao , R.R., R.L.Mauck , W. Liu, W.B. Valhmu, C.T. Hung *Chondrocyte Translocation Response to Direct Current Electric Fields*. Journal of Biomechanical Engineering, 2000. **122**: p. 261-267.
34. Takao Inoue, H.O., *A New Drying Method of Biological Specimens for Scanning Electron Microscopy The t-Butyl Alcohol Freeze-drying Method*. Arch. Histol. Cytol., 1988. **51**(1): p. 53-59.
35. Roeder, B.A., et al., *Tensile Mechanical Properties of Three-Dimensional Type I Collagen Extracellular Matrices With Varied Microstructure*. Journal of Biomechanical Engineering, 2002. **124**(2): p. 214.

36. Li, Q., Lau, Anthony, Morris, Terence J., Guo, Lin, Fordyce, Christopher B., Stanley, Elise F. , *A Syntaxin 1, G $\alpha$ o, and N-Type Calcium Channel Complex at a Presynaptic Nerve Terminal: Analysis by Quantitative Immunocolocalization*. Journal of Neuroscience, 2004. **24**: p. 4070-4081.
37. Sander E. A, B.V.H., *Comparison of 2D fiber network orientation measurement methods*. J Biomed Mater Res A, 2009. **88**(2): p. 322-331.
38. Matthews JA, W.G., Simpson DG, Bowlin GL., *Electrospinning of collagen nanofibers*. Biomacromolecules, 2002. **3**: p. 232–238.
39. R. B.Dickinson, S.G., R. T. Tranquillo, *Biased cell migration of fibroblasts exhibiting contact guidance in oriented collagen gels*. Ann. Biomed. Eng. , 1994. **22**: p. 342-356.
40. Wilson DL, M.R., Hong S, Cronin-Golomb M, Mirkin CA, Kaplan DL. , *Surface organization and nanopatterning of collagen by dip-pen nanolithography*. Proc Natl Acad Sci U S A 2001. **98**: p. 13660–13664.
41. K.A.Faraj, T.H.v.K., W.F.Daamen *Construction of collagen scaffolds that mimic the three-dimensional architecture of specific tissues*. . Tissue Eng, 2007. **13**: p. 2387–2394.
42. David Vader, A.K., David Weitz, Lakshminarayana Mahadevan, *Strain-Induced Alignment in Collagen Gels*. PLoS ONE, 2009. **4**(6): p. 1-12.
43. Dallon, J.C. and H.P. Ehrlich, *A review of fibroblast-populated collagen lattices*. Wound Repair and Regeneration, 2008. **16**(4): p. 472-479.
44. Irina Kaverina, O.K., J. Victor Small, *Microtubule Targeting of Substrate Contacts Promotes Their Relaxation and Dissociation*. The Journal of Cell Biology, 1999. **146**(5): p. 1033–1043.
45. Chen, B.H., *Roles of Rho-associated Kinase and Myosin Light Chain Kinase in Morphological and Migratory Defects of Focal Adhesion Kinase-null Cells*. Journal of Biological Chemistry, 2002. **277**(37): p. 33857-33863.
46. Kolega, X.L.J., *Effects of Direct Current Electric Fields on Cell Migration and Actin Filament Distribution*. J Vasc Res, 2002. **39**: p. 391-404.
47. Albert. K. Harris, N.K.P., David Paydarfar, *Effects of Electric Fields*

- on Fibroblast Contractility and Cytoskeleton*. The Journal of Experimental Zoology, 1990. **253**: p. 163-176
48. G.Totsukawa, *Distinct roles of MLCK and ROCK in the regulation of membrane protrusions and focal adhesion dynamics during cell migration of fibroblasts*. The Journal of Cell Biology, 2004. **164**(3): p. 427-439.
49. Brown, T.D., *Techniques for mechanical stimulation of cells in vitro: a review*. Journal of Biomechanics, 2000. **33**(1): p. 3-14.
50. E. Cukierman, R.P., K. M. Yamada, *Cell interactions with three-dimensional matrices*. Current Opinion in Cell Biology, 2002. **14**(5): p. 633-640.



## Appendix

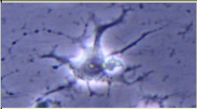

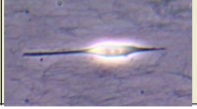
Drug	Morphology	Working Concentration	Directionality	Migration Speed
C3 (Rho ↓ )		2.0 µg/ml (Serum free, 4hr)	—	↓
NO <sub>2</sub> Try (Destablize microtubule)		400µM (Medium, 24hr)	—	↓
LPA (Rho ↑ )		10µM (Medium, 4hr)	↑	—

Chart of other pharmacological drugs tested on EF cell migration. 2D thin aligned collagen matrix was used in EF cell migration experiments listed above. C3 (cytoskeleton), NO<sub>2</sub>Tyr (3-nitrotyrosine, Sigma) and LPA (L- $\alpha$ -lysophosphatidic acid, Sigma) were used.

